

Cytotoxic effects of the cardenolide convallatoxin and its Na,K-ATPase regulation

Naira Fernanda Zanchett Schneider¹ · Izabella Thais Silva¹ · Lara Persich¹ · Annelise de Carvalho¹ · Sayonarah C. Rocha² · Lucas Marostica¹ · Ana Carolina Pacheco Ramos² · Alex G. Taranto³ · Rodrigo M. Pádua⁴ · Wolfgang Kreis⁵ · Leandro A. Barbosa² · Fernão C. Braga⁴ · Cláudia M. O. Simões¹

Received: 3 August 2016 / Accepted: 21 December 2016 / Published online: 7 February 2017
© Springer Science+Business Media New York 2017

Abstract Cardenolides are cardiac glycosides, mostly obtained from natural sources. They are well known for their inhibitory action on the Na,K-ATPase, an effect that regulates cardiovascular alterations such as congestive heart failure and atrial arrhythmias. In recent years, they have also sparked new interest in their anticancer potential. In the present study, the cytotoxic effects of the natural cardenolide convallatoxin (CON) were evaluated on non-small cell lung cancer (A549 cells). It was found that CON induced cytostatic and cytotoxic effects in A549 cells, showing essentially apoptotic cell death, as detected by annexin V-propidium iodide double-staining, as well as changes in cell form. In addition, it prompted cell cycle arrest in G2/M and reduced cyclin B1 expression. This

compound also increased the number of cells in subG1 in a concentration- and time-dependent manner. At a long term, the reduction of cumulative population doubling was shown along with an increase of β -galactosidase positive cells and larger nucleus, indicative of senescence. Subsequently, CON inhibited the Na,K-ATPase in A549 cells at nM concentrations. Interestingly, at the same concentrations, CON was unable to directly inhibit the Na,K-ATPase, either in pig kidney or in red blood cells. Additionally, results of docking calculations showed that CON binds with high efficiency to the Na,K-ATPase. Taken together, our data highlight the potent anticancer effects of CON in A549 cells, and their possible link with non-classical inhibition of Na,K-ATPase.

Electronic supplementary material The online version of this article (doi:10.1007/s11010-016-2914-8) contains supplementary material, which is available to authorized users.

✉ Cláudia M. O. Simões
claudia.simoes@ufsc.br

¹ Departamento de Ciências Farmacêuticas, Centro de Ciências da Saúde, Universidade Federal de Santa Catarina (UFSC), LVA, CIF, CCS, Florianópolis,, SC 88040-900, Brazil

² Laboratório de Bioquímica Celular, Campus Centro-Oeste Dona Lindu, Universidade Federal de São João del Rei, Divinópolis, MG, Brazil

³ Laboratório de Bioinformática, Campus Centro Oeste Dona Lindu, Universidade Federal de São João Del Rei, Divinópolis, MG, Brazil

⁴ Departamento de Produtos Farmacêuticos, Faculdade de Farmácia, Universidade Federal de Minas Gerais, Belo Horizonte, MG, Brazil

⁵ Department of Biology, Friedrich-Alexander Universität, Erlangen, Germany

Keywords Cardenolides · Convallotoxin Convallatoxin · Cytotoxic effects · A549 cells · Apoptosis · Na,K-ATPase

Abbreviations

CON	Convallatoxin
NSCLC	Non-small cell lung cancer
PAC	Paclitaxel
FBS	Fetal bovine serum
TB	Trypan blue
NII	Nuclear irregularity index
SDS	Sodium dodecyl sulfate
DOC	Deoxycholate
EDTA	Ethylenediaminetetraacetic acid
RIPA	Radioimmunoprecipitation assay buffer
PVDF	Polyvinylidene fluoride
DAPI	4',6-Diamidino-2-phenylindole
EGTA	Ethylene glycol tetraacetic acid
FACS	Fluorescence-activated cell sorting.

Introduction

Lung cancers are the leading cause of cancer deaths worldwide, with non-small cell lung cancer (NSCLC) representing the majority of cases [1]. Although NSCLC chemotherapy uses a variety of drugs with distinct mechanisms of action, the overall survival rate is low [2]. In addition, cell death resistance is a limiting factor in the therapeutic effects of a drug, leading to drug resistance [3]. Therefore, the search for new anticancer agents, especially with different mechanisms of action from those clinically available, remains an important goal to be followed.

Most of the anticancer agents in clinical use are natural products or derivatives. In this context, marine and terrestrial organisms are considered important sources for novel lead compounds. Some of the well-known plant-derived anticancer drugs in clinical use are the vinca alkaloids vincristine and vinorelbine, isolated from *Catharanthus roseus*; etoposide and teniposide, which are semisynthetic derivatives of the natural lignan podophyllotoxin; and paclitaxel and docetaxel, which are derived from the *Taxus* species [4, 5].

In recent years, cardenolides mainly obtained from *Digitalis lanata*, *D. purpurea*, and *Convallaria majalis* have been shown to present anticancer potential [reviewed in: 6–9]. In vitro and in vivo approaches have revealed that some cardenolides (e.g., digoxin, digitoxin, oleandrin, ouabain, and UNBS1450) present potent and selective anticancer properties [10–16].

The anticancer potential of convallatoxin (CON) (Fig. 1a), a well-known cardenolide with one L-rhamnose sugar, has been investigated in vitro against different cancer cells (e.g., colorectal [11], lung [17], cervical, fibrosarcoma, liver [18], breast [19], and pancreatic [20]), with promising results.

The cytotoxic effects of cardenolides have been correlated with the inhibition of Na,K-ATPase, a transmembrane antiport ion transporter that pumps three sodium out and two potassium into the cell membrane against their concentration gradients [21]. Na,K-ATPase exists as heterodimer conformations in the cell membrane, with equimolar amounts of the α and β subunits. A γ subunit is also encoded by the FXYD2 gene and forms part of the Na,K-ATPase in some tissues [22]. The α subunit has a molecular weight of 112 kDa and is the catalytic subunit of the enzyme that contains the domains to binding Na^+ , K^+ , ATP as well as cardenolides. Four different isoforms have been described for the α subunit: $\alpha 1$, which is ubiquitously expressed across the tissues; $\alpha 2$, which is expressed in muscle, adipocyte, heart, and brain; $\alpha 3$, which is expressed mainly in brain; and $\alpha 4$, which is expressed in testis cells [23]. Moreover, these isoforms exhibit different sensitivities to cardenolides, which is dependent on two amino acid

modifications in the first extracellular region of the $\alpha 1$ subunit. The $\alpha 1$ subunit in rodents is essentially cardenolide insensitive, showing ~1000-fold less sensitivity than the human subunit, whereas in humans, all isoforms present the same sensitivity to cardenolides [9]. In addition to its ion-translocating function, this protein complex may act as a receptor for cardenolide-activating intracellular signaling pathways, eliciting marked effects on cancer cell behavior. The most probable pathways include the involvement of Na,K-ATPase in cell adhesion, invasion, metabolism, and death [21, 24–26].

Although previous reports have addressed the cytotoxic effects of cardenolides, the investigation of their distinct mechanisms of cell death and their relationship with the possible membrane targets in different cancer cells has not yet been explored [8]. Additionally, few of these works have given special attention to CON. In this context, we herein describe, for the first time, the cytotoxic and cytostatic effects prompted by CON in A549 cells, including its mechanism of cell death and cell cycle modulation. These data were also linked to the effects of CON on Na,K-ATPase, the main target membrane of cardenolides.

Materials and methods

Cardenolides, chemicals, and cells

Convallatoxin, the positive control paclitaxel (PAC) and the inhibitor chloroquine (CQ) were purchased from Sigma-Aldrich, St. Louis, MO, USA. Prior to dilution in culture medium, these samples were dissolved in dimethyl sulfoxide (DMSO) (Merck Millipore, Billerica, MA, USA). Caspase inhibitor (z-VAD-FMK) was also purchased from Merck.

Human NSCLC cells (A549 cells, ATCC: CCL185) were grown in Minimal Essential Medium (MEM; Cultilab, Campinas, SP, Brazil) supplemented with 10% fetal bovine serum (FBS; Gibco, Carlsbad, CA, USA) and maintained at 37 °C in a humidified incubator under 5% CO_2 /95% air. Cells were maintained free of antibiotics, and were routinely screened for microorganisms, including mycoplasma.

Cell viability assessment

Trypan blue (TB) staining was used to evaluate A549 cell viability [27]. Cells (5×10^5 /well in 6-well plates) were treated with CON up to 24, 48, and 72 h. Cells were then harvested by trypsinization and TB dye was added to the cell suspensions. Total cells (viable and non-viable) were counted on a Countess™ automated cell counter (Invitrogen, Carlsbad, CA, USA). Data were normalized to the

control and reported as number of cells and percentage of TB-positive cells.

Clonogenic assay

The clonogenic assay was performed according to Franken [28]. A549 cells (5×10^2 cells/well in six-well plates) were incubated at 37 °C for 24 h. Thereafter, treatment with CON at various concentrations was performed for 48 h. The medium was then removed, and cells received fresh medium supplemented with 10% FBS for 10 days. The medium was replaced every 3 days. After this period, the colonies were stained with crystal violet and counted using a stereomicroscope (Olympus, Center Valley, PA, USA).

Cell form analyses

To evaluate the cell form alterations, A549 cells were seeded in 12-well plates and treated with CON (10 and 100 nM) and PAC (100 nM) for 48 h. After treatment, the cells were fixed and incubated with TRITC-labeled-phalloidin (Invitrogen, Carlsbad, USA) for F-actin staining. Fluorescence images were obtained using a Olympus FluoView™ 1000, Hicksville, NY, USA from the Microscopy Center of the Federal University of Rio Grande do Sul (UFRGS) and brightness-contrast images were obtained using a BX-41 inverted microscope (Olympus).

Nuclear form analyses

As described in “Cell form analyses” section, fixed cells were further DAPI-stained in 0.1% Triton X-100 (v/v in PBS) for 20 min at room temperature. To verify the influence of caspases, their inhibitor z-VAD was used in co-treatment with CON at 100 nM. Nuclei images were taken and quantified using the Software Image J 1.50i (National Institutes of Health, Bethesda, USA) and the plugin “NII_Plugin” is available at <http://www.ufrgs.br/labsinal/NMA/>. Data were presented as a plot of Area versus nuclear irregularity index (NII), which separates nuclei by their morphometric phenotype. The percentages of normal, large regular, and small regular nuclei were determined as described [29].

Flow cytometry for cell cycle analyses

A549 cells were treated with CON for 24, 48, and 72 h, and the effects on cell cycle were evaluated by propidium iodide staining (PI—Sigma—Aldrich), as previously described [30]. Flow cytometry analyses were performed on a fluorescence-activated cell sorting (FACS) Canto II cytometer [Becton Dickinson (BD) GmbH, Heidelberg, Germany] and the events were acquired for each group.

The population of cells in each phase of the cell cycle was determined using the free software Flowing 2.5.0 (University of Turku, Finland).

Flow cytometry for apoptosis analyses

A549 cells were treated with CON for 12 and 48 h, and then subjected to the annexin V-FITC Apoptosis Detection Kit (Sigma—Aldrich) [31]. Data were obtained with a FACS Canto II cytometer, and analyses were performed using the software Flowing 2.5.0. Camptothecin (5 μM) (Sigma—Aldrich) was used as positive control for apoptosis, and a pellet of cells freezing (−80 °C)/defrosting (56 °C) was used as necrosis control. Apoptotic cells were identified by annexin V—propidium iodide double-staining.

Long-term culture of A549 cells treated with CON and determination of population doublings

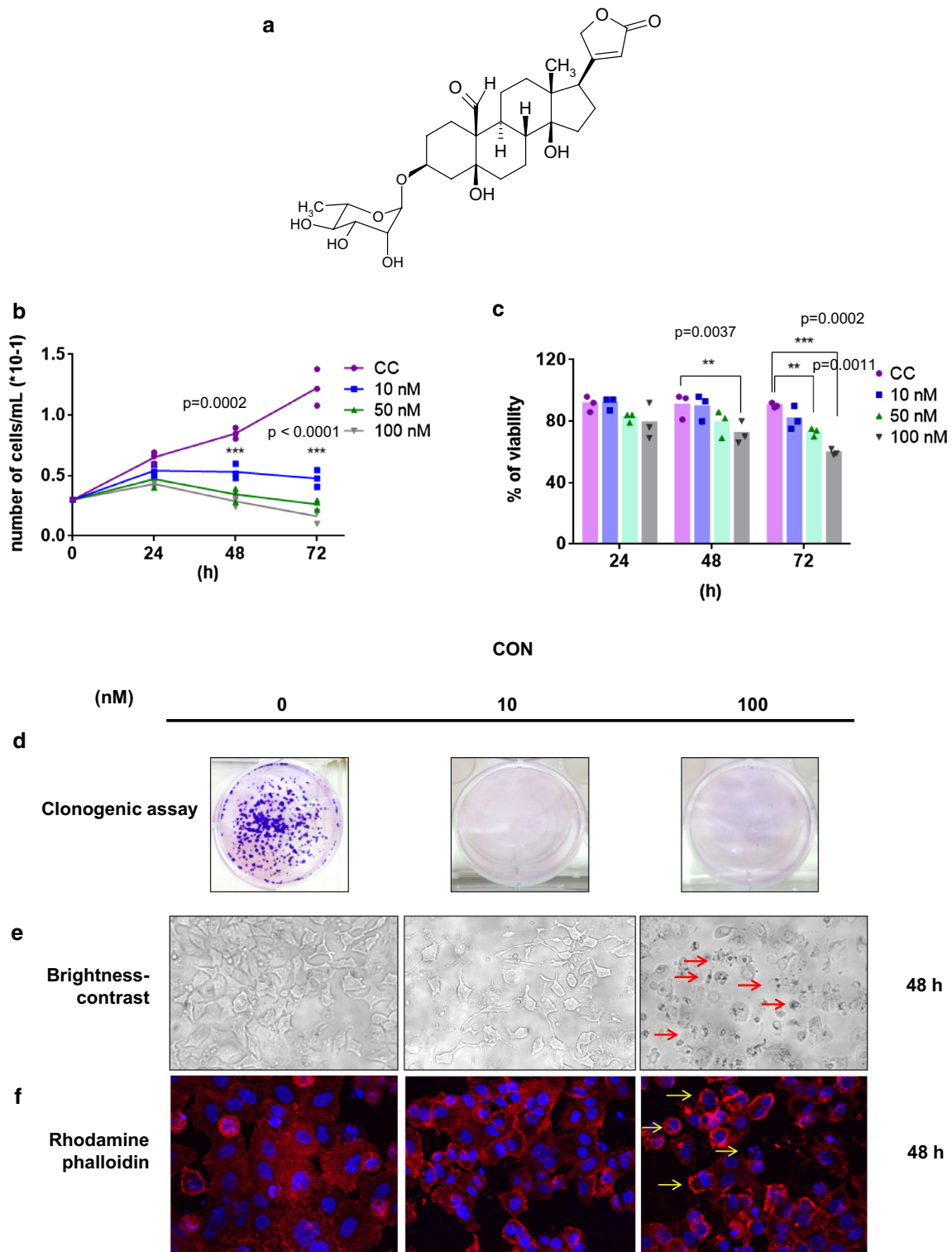
The long-term analysis was performed according to Silva et al. [32]. Cells were plated in 12-well plates at a density of 2×10^4 cells/well and exposed to CON at 10 and 50 nM, renewing the medium every 72 h. Treatments with a minimum 20% and a maximum 80% of cells confluence were trypsinized, and population doublings (PD) were determined according to the formula $PD = [\log N(t) \times \log N(to)] / \log 2$, where $N(t)$ is the number of cells per well at time of passage and $N(to)$ is the number of cells seeded in the previous passage. The sum of PDs was then plotted against the culture time. After all, the cells were stained with SA-β-gal (Materials and Methods “Senescence-associated-β-galactosidase (SA-β-gal) staining”) and DAPI, as shown in Materials and Methods “Nuclear form analyses”.

Senescence-associated-β-galactosidase (SA-β-gal) staining

After long-term treatment (15 days), cells were washed with PBS, fixed in paraformaldehyde 4% for 15 min at room temperature, washed, and incubated with fresh SA-β-gal staining solution (1 mg/mL X-gal (Sigma—Aldrich), 40 mM citric acid/sodium phosphate (pH 6.0), 5 mM potassium ferrocyanide, 5 mM potassium ferricyanide, 150 mM NaCl, and 2 mM MgCl) for 12 h at 36 °C. The results were presented as the ratio of SA-β-gal-positive cells to total cells of three independent experiments.

Molecular modeling analyses

The CON analog was generated using MarvinSketch (MarvinSketch. [<http://www.chemaxon.com/marvin/sketch/index.jsp>]). Next, CON was refined using the semi-empirical parametric method 7 (PM7) [33] implemented on



MOPAC software [34]. Gasteiger charges were then added to CON and the molecular target 4HYT [35] using the AutoDock Tools software [36]. A grid box was generated to cover the entire binding site with x, y, z $-27.065, 20.469, -69.469$ Å. The validation redocking step was performed

according to a previous study [37]. Finally, the docking process was performed using AutoDock Vina, with exhaustiveness set to 20 [38]. The docking results were analyzed using Discovery Studio 4.5 [39].

Fig. 1 CON induced cytotoxic effects in A549 cells. **a** Chemical structure of convallatoxin. **b** Growth inhibition of A549 cells by CON expressed as number of cells after 24, 48, and 72 h of treatment obtained by the Trypan blue assay. The data shown represent the scatter plot (+bars representing the mean of three independent experiments) $***p < 0.001$ (ANOVA followed by Dunnett's test) when compared to the untreated control (CC). **c** Effects of CON on A549 cell viability. The viability was normalized as a percentage of cells and represented as scatter plot (+bars representing the mean of three independent experiments). $**p < 0.01$ and $***p < 0.001$ (ANOVA followed by Dunnett's test) when compared to the untreated control (CC). **d** CON reduced clonogenic survival. After 48 h of CON treatment, cells were washed with warm PBS, received fresh medium and were allowed to grow for 10 days. Colonies of A549 cells were measured by staining them with crystal violet. The images shown represent the mean \pm SD of three independent experiments. **e** A549 cell form changes in cells treated with CON at 10 and 100 nM for 48 h. Images were captured by a phase-contrast microscope, 400 \times . Red arrows indicate form changes in relation to the control. The images shown are representative of three independent experiments. **f** F-actin staining with rhodamine phalloidin and DAPI of A549 cells after CON treatment and captured by a fluorescence microscope, 400 \times . Yellow arrows indicate changes in cytoskeletal form in relation to the control. The images shown are representative of three independent experiments. (Color figure online)

Fractionation of cell lysates and preparation of membrane fractions

A total of 3.0×10^5 cells were grown in 75 cm² culture flasks and treated with CON (5, 10, and 50 nM). After 48 h of treatment, cells were washed with PBS and removed by scrapping the surface of the culture flask in a membrane preparation buffer [6 mM Tris (pH 6.8), 20 mM imidazole, 0.25 M sucrose, 0.01% SDS, 3 mM EDTA, and 1/1000 protease inhibitor]. Cells were homogenized in a potter–Elvehjem system (Nova Técnica, Piracicaba, SP, Brazil), for twenty stokes in ice. This step was followed by centrifugation at 4000 $\times g$ for 10 min at 4 °C (Eppendorf, Hamburg, Germany). Next, the supernatant was subjected to centrifugation at 20,000 $\times g$ for 90 min at 4 °C. Finally, the pelleted membrane fraction was resuspended in 150 μ L of membrane preparation buffer.

The purified Na,K-ATPase was prepared from pig kidney outer medulla as proposed by Jørgensen [40], with the modifications described by Jensen, Nørby, and Ottolenghi [41]. The stock preparations were kept at -20 °C in storage buffer (12.6 mM imidazole, 0.625 mM EDTA, 250 mM sucrose, titrated to pH 7.4 with HCl). The ATPase activity at 37 °C was in the range of 6–20 μ mol $\text{mg}^{-1} \text{min}^{-1}$, values compatible with fully functional preparations.

Preparations of human erythrocyte cytoplasm-free membrane ghosts were performed according to Sousa and coworkers [42]. Briefly, the blood concentrates were spun at 6500 $\times g$ for 10 min at 4 °C. The precipitates were dissolved in a solution of 20 mM Tris–HCl (pH 7.4), 130 mM KCl, and 0.6 mg/ml phenylmethylsulfonyl fluoride (PMSF). This

suspension was spun at 6500 $\times g$ for 10 min at 4 °C. The cells were submitted to lysis by freezing in liquid nitrogen followed by thawing at room temperature (25 °C). The lysates were then mixed with 5 mM 4-2-hydroxyethyl-1-piperazineethanesulfonic acid (HEPES; pH 7.4), 1 mM ethylenediamine tetraacetic acid (EDTA), and 0.6 mg/ml PMSF and spun again at 9,000 $\times g$ for 10 min at 4 °C. This centrifugation step was repeated four times; the resulting pellet was dissolved in 10 mM HEPES (pH 7.4), 130 mM KCl, 0.5 mM MgCl_2 , and 0.05 mM CaCl_2 , and finally spun at 9000 $\times g$ for 10 min, mixed with a small volume of this last buffer, and stored in nitrogen until use.

Measurement of CON effects on Na,K-ATPase activity

Na,K-ATPase activity was measured using two membrane preparation approaches. Firstly, membrane fractions from A549 cells were prepared as described in item 2.8. A549 cells membrane preparations (15 μ g of protein) were incubated at 37 °C for 1 h in 120 mM NaCl, 20 mM KCl, 2 mM MgCl_2 , 3 mM ATPNa_2 , and 50 mM HEPES, (pH 7.5). Secondly, The purified Na,K-ATPase (9.6 μ g of protein) or erythrocyte ghost membranes (23 μ g of protein) were incubated at 37 °C for 20 min in medium containing 130 mM NaCl, 20 mM KCl, 40 mM Tris–HCl (pH 7.4), and 5 mM MgCl_2 . Both experiments of membrane preparations were evaluated in the absence or presence of ouabain (1 mM) and increasing concentrations of CON. The Na,K-ATPase activity was determined by measuring the P_i released, using a previously described colorimetric method [43], and specific activity was considered as the difference between the total and ouabain-resistant ATPase activities [44].

Western blot analyses

A549 cells (5.0×10^5 /well in six-well plates) were treated with CON at 10 and 100 nM for 24 h or 48 h. Whole cells were harvested after lysis with RIPA lysis buffer (25 mM Tris–HCl pH 8.0, 137 mM NaCl, 10% glycerol, 0.1% SDS, 0.5% DOC, 1% NP40, 2mM EDTA pH 8.0, 5 mg ml^{-1} leupeptin, 5 mg ml^{-1} aprotinin, 0.2 mM Pefabloc, 1 mM sodium vanadate, and 5 mM benzamide) and centrifuged at 10,000 $\times g$ for 20 min, at 4 °C. Protein concentration was determined by the Bradford assay (kit from Bio-Rad, Hercules, USA). Equivalent amounts of protein were separated on a 10% sodium dodecyl sulfate polyacrylamide gel electrophoresis (SDS–PAGE) followed by electron transfer to PVDF membranes (Millipore, Darmstadt, HE, Germany). After blocking with 5% non-fat milk in PBS Tween, membranes were incubated overnight at 4 °C with cyclin B1 antibody or LC3B (Cell Signaling Technology, Danvers, MA, USA). After incubation with the corresponding secondary antibody conjugated to horseradish peroxidase,

protein bands were revealed by Pierce Enhanced Chemiluminescence ECL substrate (Thermo Scientific, MA, USA) using a ChemiDoc MP device (Bio-Rad). An antibody against β -actin (Sigma–Aldrich) was used as control for equal loading.

Statistical analyses

The results were expressed as scatter plot (+bars representing the mean of three independent experiments) as recommended by Klaus (2016) to show small datasets (<10) [45] or stacked bars to show cell cycle data. Statistical analyses were performed by one-way ANOVA followed by the Dunnett's or Tukey's post hoc tests. GraphPad Prism 5 software (GraphPad, USA) was used to calculate all the data.

Results

CON affected A549 cells proliferation and viability

In the present study, CON was evaluated for its effects on A549 cell proliferation and viability by Trypan blue assay (Fig. 1b, c). CON reduced A549 cell numbers at all the tested concentrations after 48 h (Fig. 1b). The decrease in proliferation observed at 100 nM was accompanied by the accumulation of Trypan blue-positive cells at 48 h (Fig. 1c). Effects on cell viability were time-dependent. No significant statistical differences were observed in relation to the controls on Trypan blue-positive cells after 24, 48, and 72 h when cells were treated with CON at 10 nM. Treatment with CON at 100 nM decreased the number of viable cells in relation to the controls, within the first 48 h, reaching only 30% of cell death after 72 h.

CON inhibited A549 cell colony formation

To assess the effects of CON on the reproductive cell integrity to establish colonies, the clonogenic activity was investigated in A549 cells. Following 48 h exposure to various concentrations of this compound (0, 10, 50, and 100 nM), cells seeded in six-well plates were then incubated with free-CON media for 10 days. It was found that CON exposure leads to significant suppression of colony formation, since the lowest tested concentration (10 nM) almost completely abolished the clonogenic capacity. Colonies with more than 50 cells were not observed at all the concentrations tested (Fig. 1d).

CON exposure caused cell form changes in A549 cells

In order to verify the cell form features after CON exposure, brightness–contrast images were taken after 48 h of

treatment. As shown in Fig. 1e, cells treated with CON at 100 nM for 48 h showed the typical appearance of apoptotic cells, such as cell shrinkage and apoptotic bodies under a phase-contrast microscope, as shown for PAC (Supplementary data, Fig. S1). In Fig. 1f, rhodamine phalloidin staining showed that CON treatment induced partial disorganization and disruption of the actin stress fibers.

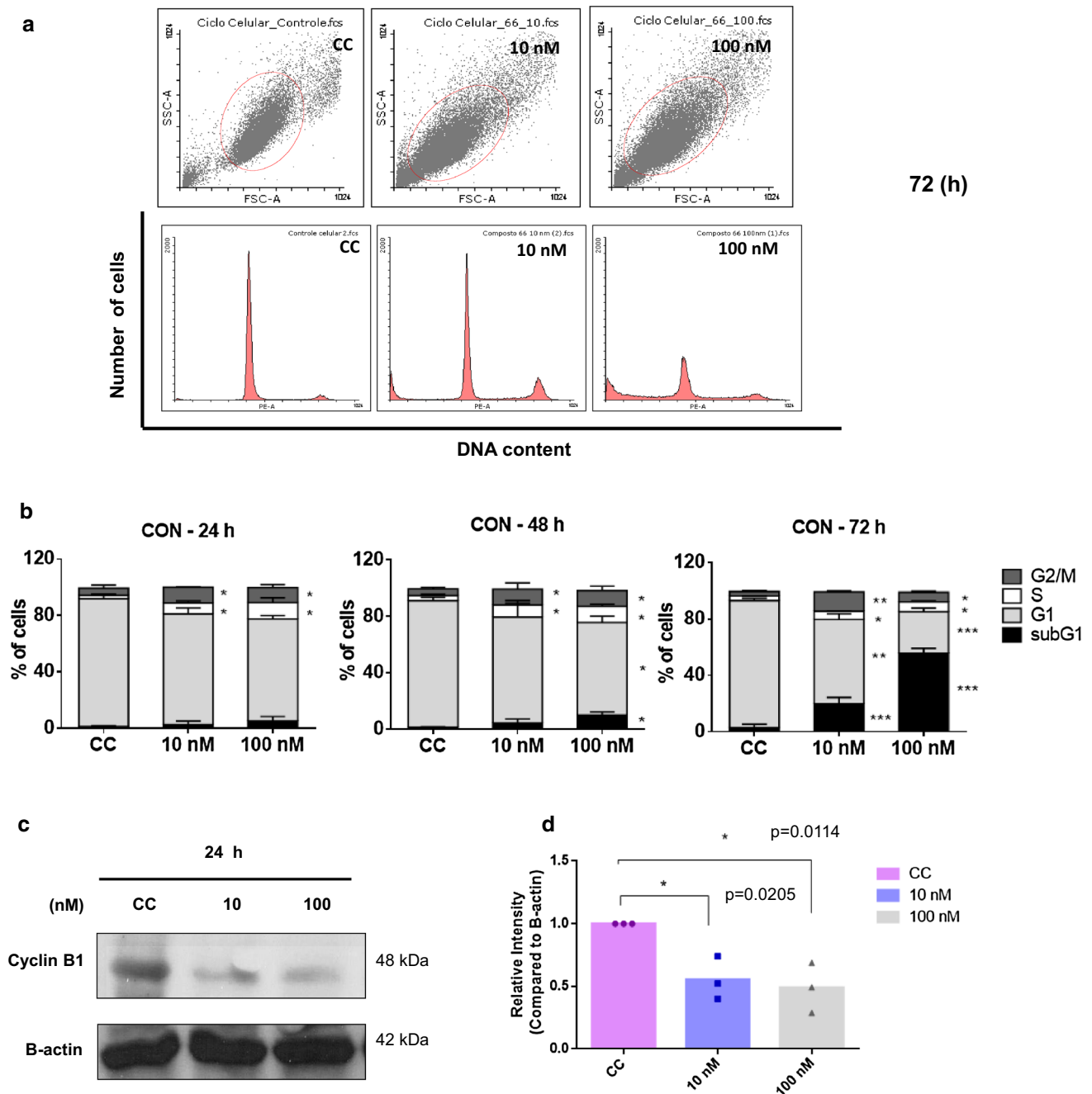
CON induced cell cycle arrest and down-regulated cyclin B1 expression

To further investigate the growth inhibition potential of CON in A549 cells, the effects on cell cycle progression were evaluated by FACS analyses. Cell distribution after 24, 48, and 72 h of CON treatment was different from that of the untreated controls, as observed in Fig. 2a, b. Exposure of A549 cells to CON at 10 and 100 nM showed a significant increase in cells in the G2/M phase at all times tested, followed by an increase in cells in subG1 over the time.

We also evaluated the expression of a key molecular driver of G2/M phase, cyclin B1, after 24 h of treatment by WB analysis. Figure 2c, d shows that CON down-regulates cyclin-B1.

Nuclear form analyses of A549 cells

Since CON treatment resulted in a significant decrease in cell viability, as well as enhancement of cells in subG1 and form changes, we wondered whether it would induce apoptosis. Initially, cell death was measured in A549 cells by microscopic observation of nuclear form upon staining with the nuclei dye DAPI. Cells untreated or treated with CON for 24, 48, and 72 h were incubated with DAPI for 15 min at 37°C, and the nuclear form was observed by fluorescence microscopy (Fig. 3a). The images were captured and analyzed by nuclear morphometric analysis (NMA) (Fig. 3b). The morphometric analysis of nuclei size and irregularity showed that CON at 100 nM increased the percentage of small and regular nuclei, characteristic of apoptosis (Fig. 3c). To verify the involvement of caspases, at the same concentration of CON (100 nM) that caused significant induction of cell death, cells were co-treated with the pan caspase inhibitor z-VAD. In this condition, small and regular nuclei almost disappeared, showing that CON effects in A549 cells are caspase-dependent. Cells with irregular nuclei (large and small) comprised less than 2%, and are not shown in the graph. PAC was used as positive control and showed a high percentage of fragmented and shrunken nuclei (Supplementary Material, Fig. 1).



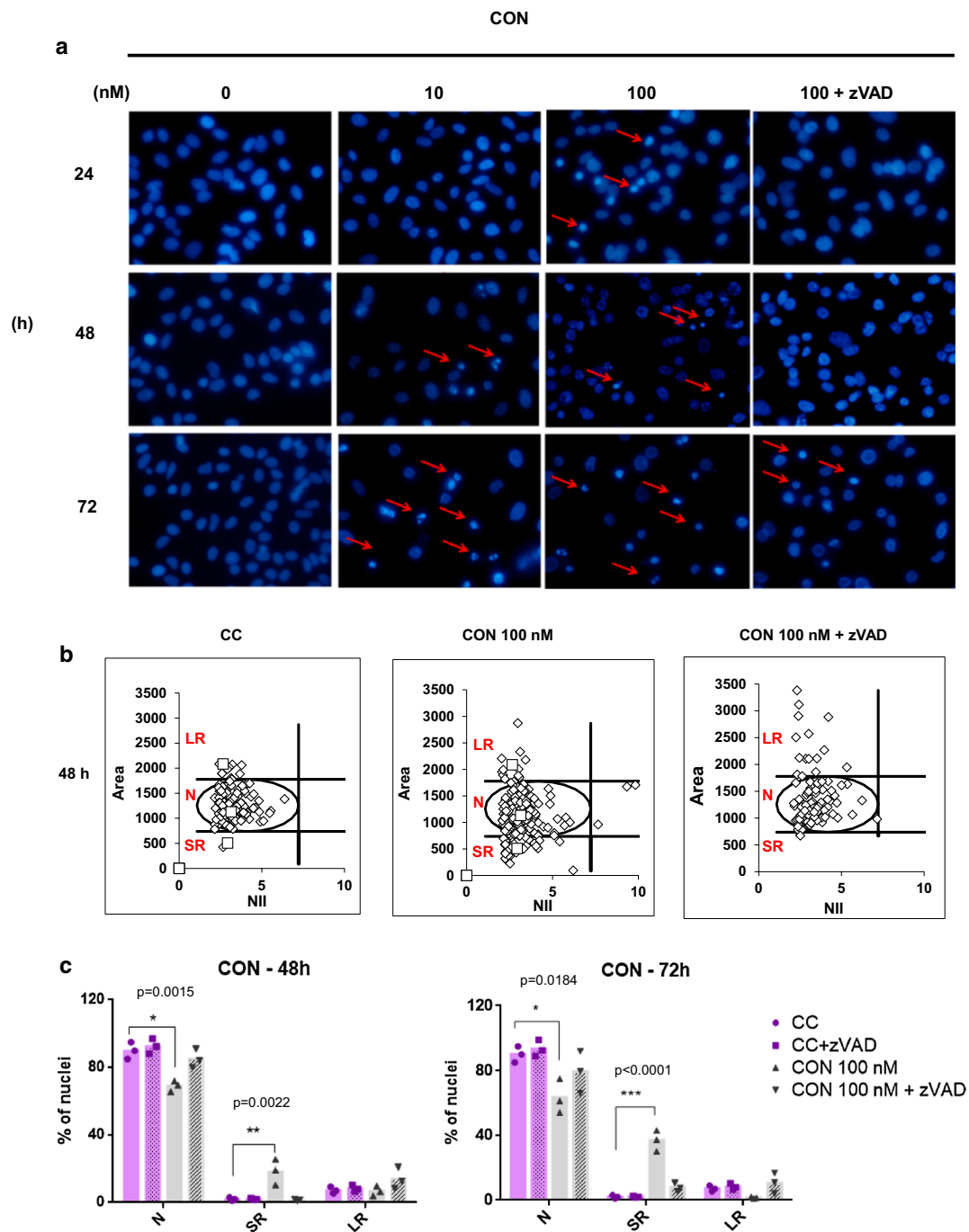


Fig. 3 CON induced apoptotic cell death. **a** A549 cells were stained with DAPI in order to detect nuclear form. Cells treated with CON (10 and 100 nM) for 24, 48, and 72 h were photographed and analyzed. *Red arrows* indicate shrunken and fragmented nuclei. 400 \times . **b** The data were presented as a plot of area versus nuclear irregularity index (NII), which separates nuclei by their morphometric phenotypes. *Letters* represent normal (N), large regular (LR), and small regular (SR) nuclei. **c** The data shown are represented as scatter plot (*+bars* representing the mean of three independent experiments). $**p < 0.01$ and $***p < 0.001$ (ANOVA followed by Dunnett's test) when compared to the untreated control (CC). **d** A549 cells were stained with annexin V-FITC and PI, following treatment

with CON, and analyzed by flow cytometry. In each panel, the lower left quadrant shows cells that are negative for both annexin V-FITC and PI; the lower right quadrant shows annexin V positive cells, which are in the early stage of apoptosis; the upper left shows PI positive cells, which are dead; and upper right shows both annexin V and PI positive cells, which are in the late stage of apoptosis. **e** Percentages of annexin V positive cells (early and late apoptosis) after 12 and 48 h of CON treatment. The data shown are represented as scatter plot (*+bars* representing the mean of three independent experiments). ($**p < 0.01$, ANOVA followed by Dunnett's test) when compared to the untreated control (CC). (Color figure online)

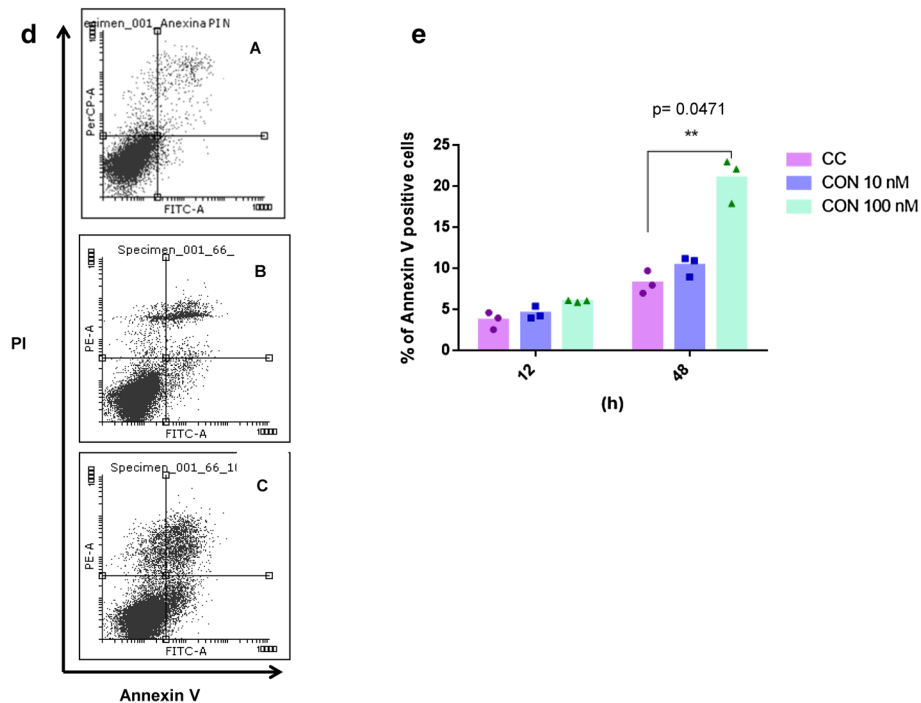


Fig. 3 (continued)

Evaluation of apoptosis

To confirm the induction of apoptosis observed by nuclei shrinkage, annexin V-FITC/PI double-staining was performed. A549 cells were treated with CON for 12 and 48 h. Fig. 3d shows four sets of populations: unstained viable cells, early apoptotic cells (annexin V positive), necrotic cells (PI positive cells), and late apoptotic cells (annexin V and PI positive cells). CON treatment (100 nM) led to a significant increase in the population of cells undergoing apoptosis after 48 h of treatment (Fig. 3e).

CON affected A549 cells at long-term treatment

Further experiments were conducted to determine if long-term treatment with CON would affect A549 cell proliferation. These cells were treated for 48 h, followed by CON-free medium for 14 days. CON reduced the number of CPD in comparison to the control at 10 nM (Fig. 4a); however, the cells maintained their proliferative potential. At 50 nM, few cells survived until the end of the experiment (less than 10% confluence) making impossible to count CPD. Additionally, after this period, cells were stained to evaluate nuclear form and SA- β -gal-positive cells (Fig. 4b). CON induced at 50 nM an increase of \sim 80% of β -gal-positive cells (Fig. 4c). At 10 nM, an increase of larger regular nuclei (Fig. 4d, e) was observed as well as the cells become

flat, increase their volume and display a vacuole-rich cytoplasm, characteristic of senescence.

CON effects on Na,K-ATPase activity

Figure 4 shows the ability of CON to inhibit the Na,K-ATPase isolated both from pig kidney (Fig. 5a) and human erythrocytes (Fig. 5b). The most significant inhibition was observed at the highest tested concentrations (500 nM, 1 and 10 μ M). On the other hand, when the enzyme was obtained from A549 cells treated with CON (5 nM) for 48 h, it caused a 60% decrease in Na,K-ATPase activity (Fig. 5c).

According to the docking calculation outcomes, CON was able to bind to the Na,K-ATPase through -11.3 Kcal/mol. Our previous studies showed that ouabain complex with Na,K-ATPase by -9.8 Kcal/mol. This result suggests that CON binds to the enzyme as effectively as ouabain. Figure 6 shows the complex formed between CON and the Na,K-ATPase. As can be seen, the CON complex among the domains M1, M2, M4, M5, and extracellular M7-8 transmembrane alpha-helix domains of the α 1 subunit (Fig. 6a), composed of Gln111, Asp121, Leu125, Ala323, Glu312, Phe316, Phe783, Phe786, Arg880 (Fig. 6b). In addition, Gln111 and Glu117 formed hydrogen bonds; while Leu125, Phe316, Ala323, Phe783, and Phe786 performed hydrophobic interaction (Fig. 6c). In contrast, a

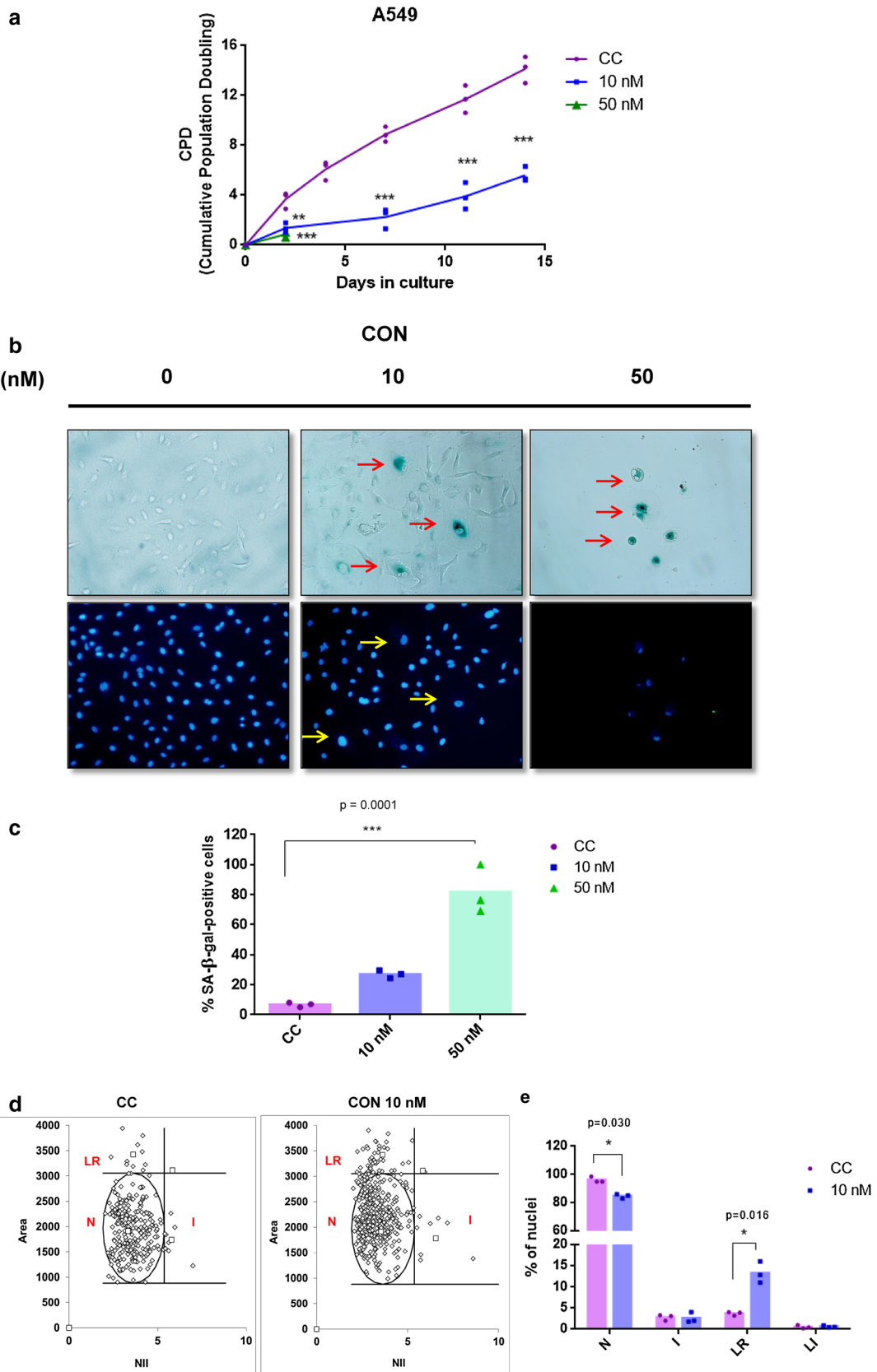


Fig. 4 Long-term effects of CON in A549 cells. **a** Cells were treated with CON (10 and 50 nM) for 48 h followed by growth in the drug-free medium for the indicated time. Cumulative population doubling (CPD) were counted. **b** After 15 days, cells were stained with SA- β -gal in order to detect senescence or DAPI in order to detect nuclear form. *Red arrows* indicate SA- β -gal-positive cells. *Yellow arrows* indicate large nuclei. The images shown are representative of three independent experiments for both conditions 400 \times . **c** percentage of SA- β -gal-positive cells. **d** DAPI stained cells were presented as a plot of Area versus nuclear irregularity index (NII), which separates nuclei by their morphometric phenotypes. *Letters* represent normal (N), irregular (I), large regular (LR), and large irregular (LI) nuclei. **e** The data shown are represented as scatter plot (+bars representing the mean of three independent experiments). (Color figure online)

steric bulk was observed for Glu312 and Arg880 against rhamnose moiety.

Discussion

In a recent publication [17], we reported that CON was one of the most effective cardenolides, among other tested cardenolides, in reducing proliferation, migration, and invasion of A549 cells. In that paper, we also showed the inhibition of proliferation of other cancer cells, such as human rhabdomyosarcoma RD, human colon carcinoma HCT-8, and human prostate carcinoma LNCaP. In previous reports, CON has been reported to be a potent cytotoxic cardenolide with IC_{50} values at nM concentration ranges, as identified herein. Its anti-proliferative effects were evaluated in cancer cells from different origins, such as colorectal (HT29, HCT116, and CC20) [11], non-small cell lung (H460 and A549) [17, 18, 46, 47], glioblastoma (U87MG) [47], cervical (HeLa) [18], liver carcinoma (HepG2) [18, 48], fibrosarcoma (HT1080) [18], pancreatic (MiaPaCa-2, BxPC-3, Panc-1, Capan-1, Su.86.86, and CFPAC-1) [20], breast (MCF-7), ovarian (1A9), kidney derived from metastatic skin (CAKI-1), skin (S-KMEL-2) [47], and prostate cell lines (DU-145) [48], and (PC3) [47]. Some of these reports also mentioned that CON was more cytotoxic to cancer cells than to non-cancerous cells [17, 18].

Although several studies have reported the anti-proliferative effects of CON in different cancer cells, few of them have investigated its effects in more detail [17, 18, 49]. In the current investigation, we focused on Na,K-ATPase and on the cytotoxic and cytostatic effects of CON in a NSCLC by various experimental approaches. Firstly, we evaluated loss of membrane integrity by TB. This assay showed that CON reduced viability in a concentration and time-dependent manner. Moreover, the clonogenic assay defines the relationship between the concentration of a drug used to produce the effects and the fraction of cells that retain their ability to reproduce. Herein, we show that CON was able to inhibit the clonogenic capacity of A549 cells. Kaushik and

coworkers (2016) also showed CON effects on clonogenic survival in NSCLC, H460 cells. They showed that CON at 25 nM almost completely abolished the clonogenic capacity of these cells, similar to what we found in this study at 10 nM.

Secondly, cell cycle analyses suggested an arrest of the G2/M phase and a concentration-dependent activation of caspases, which was evidenced by cell accumulation in the subG1 phase. Several cardenolides have been demonstrated to have anti-proliferative activity via cell cycle regulation [13]. These effects are well documented, essentially suggesting the accumulation in the G2/M phase [10, 14, 50, 51], as observed in this work. These effects may precede the onset of cell death prompted by this compound [8]. In lung cancer cells (A549 and H460), the effects on cell cycle distribution of treatment with two well-known cardiac glycosides, digoxin (50 nM) and ouabain (25 nM), for 24 h, revealed no significant alterations in the G1 or S phases. A slight increase in G2/M arrest was observed in A549 cells, and a more significant G2/M arrest was shown in H460 cells [10]. Since our results showed that the percentage of cells in the G2/M phase increased upon exposure to CON, we further investigated how CON might induce G2/M phase arrest. Specifically, we examined the expression of a key molecular driver of this phase, named cyclin B1, using Western blot analyses. Cyclin-dependant kinase complexes (CDKs) are positive regulators of cell cycle progression. Especially, the complex B-CDK1 needs to be activated during the G2/M phase in order to permit cell cycle progression [52]. CON proved to down-regulate cyclin B1, similar to what was reported by Elbaz et al. (2012) for digitoxin and the synthetic analog D6-MA. Kaushik and coworkers (2016) reported that CON arrested more than 80% of H460 cells in the G0/G1 phase in dose-dependent manner. The same authors verify that CON significantly inhibits the expression of cell cycle proteins CDK4 and cyclin D1 [49].

Thirdly, to investigate whether CON mediated reduction of cell viability and increased cells in subG1, we performed the NMA and annexin V experiments. DAPI staining showed mainly condensed nuclei, with apoptosis induction being observed in A549 cells (further validated by NMA analysis and z-VAD protection). As it has been shown by CON, the externalization of phosphatidylserine is also an indicator of apoptosis [31]. Additionally, different authors showed that CON caused induction of apoptosis and autophagy in HeLa cells [18] and in H460 cells [49]. We also evaluated the possible induction of autophagy by CON; however, this was not confirmed in A549 cells (Supplementary data S2). These data indicate the ability of CON to trigger diverse pathways and to induce different mechanisms of cell death, depending on cell type. In general, cardenolides exert anti-proliferative and cytostatic effects on different cancer cell models, as also mentioned

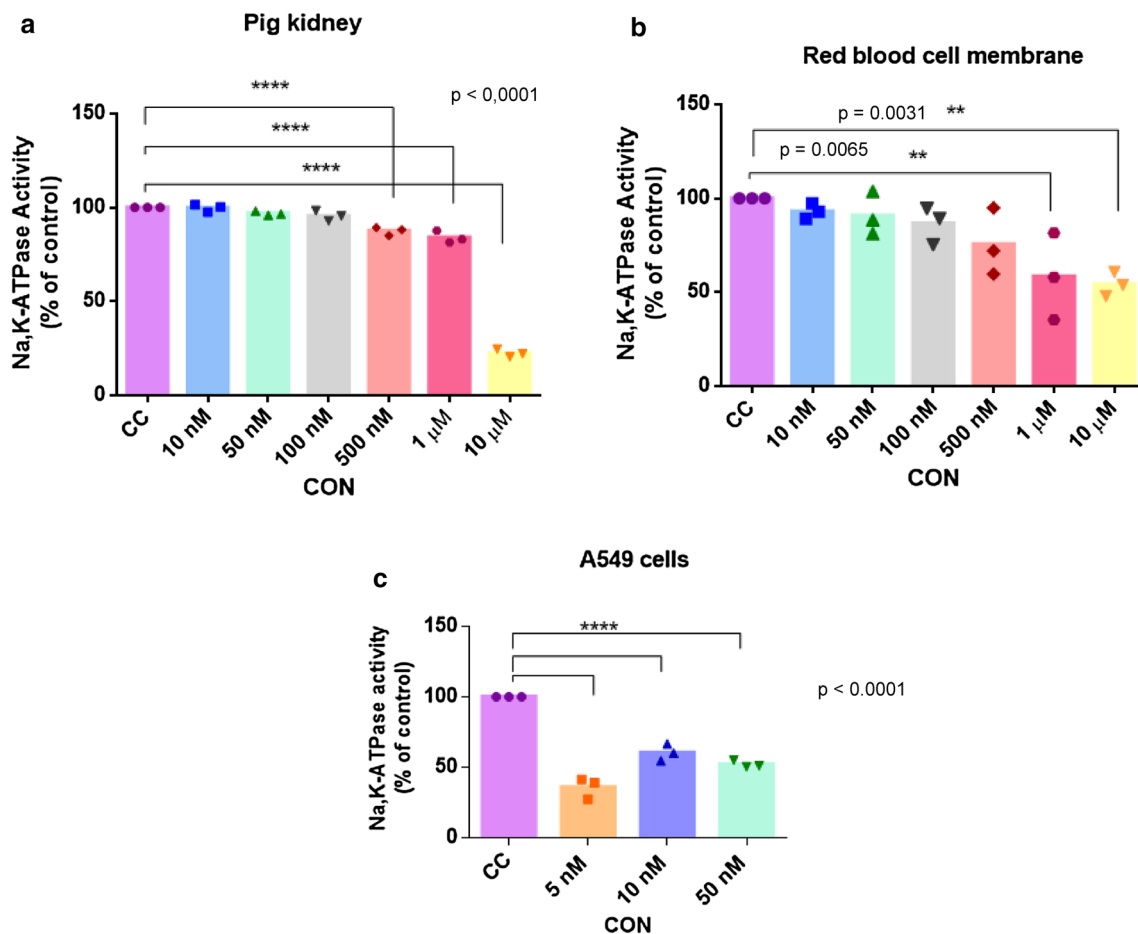


Fig. 5 Concentration–response inhibition of Na,K-ATPase activity. **a** Purified Na,K-ATPase activity from pig kidney preparation. **b** Na,K-ATPase activity of red blood cell membrane preparation. **c** Na,K-ATPase activity in A549 cells. Cells were incubated with CON for 48 h with various concentrations, and membrane preparation was

performed. The data shown are represented as scatter plot (+bars representing the mean of three independent experiments). ** $p < 0.01$, *** $p < 0.001$ and **** $p < 0.0001$ (ANOVA followed by Dunnett's test) when compared to the untreated control (CC). (Color figure online)

in this work [11, 37, 51, 53]. Their ability to reduce cancer cell viability is one of the main hallmarks of their anticancer activities. In this sense, after 48 h of treatment, CON showed a percentage of cells arrested lower than the cell number; this effect is probably caused by the induction of apoptosis in parallel with cell cycle arrest. However, besides apoptosis, different kinds of cell death might coexist in this cell population when treated with CON. Nonetheless, multiple types of cell death are triggered by these compounds, and the induction of apoptosis has been more frequently reported [18, 54–56].

After all the experiments with short duration times (~72 h), we decided to treat cells for 48 h and evaluate CON effects after long recovery times (up to 15 days). As reported by Silva and coworkers (2016), cancer is a chronic disease and needs to be evaluated also in long experimental times which may be fundamental to plan in vivo

experimental conditions. After this period, CON induced senescence in ~20% of the population at the lowest concentration tested. At 50 nM, very few cells survived and senescence can operate as a mechanism of tumor suppressor to prevent the proliferation of seriously damaged cells.

To improve the pharmacological window of CON or other cardenolides, substituents on the aglycone moiety and the stereochemical orientation may vary greatly and enrich their activity [9]. Cardenolides, such as convallatoxol and convallaside have a similar chemical structure to CON, and showed less cytotoxicity than CON among several cancer cells tested [19]. Levrier and coworkers deduced that the aldehyde group at C10 on CON plays an important role in the cytotoxic activity. However, in another study, convallatoxol, which presents an OH group instead of an aldehyde group at C10, showed strong induction of apoptosis [57]. Nonetheless, the structure–activity relationship among

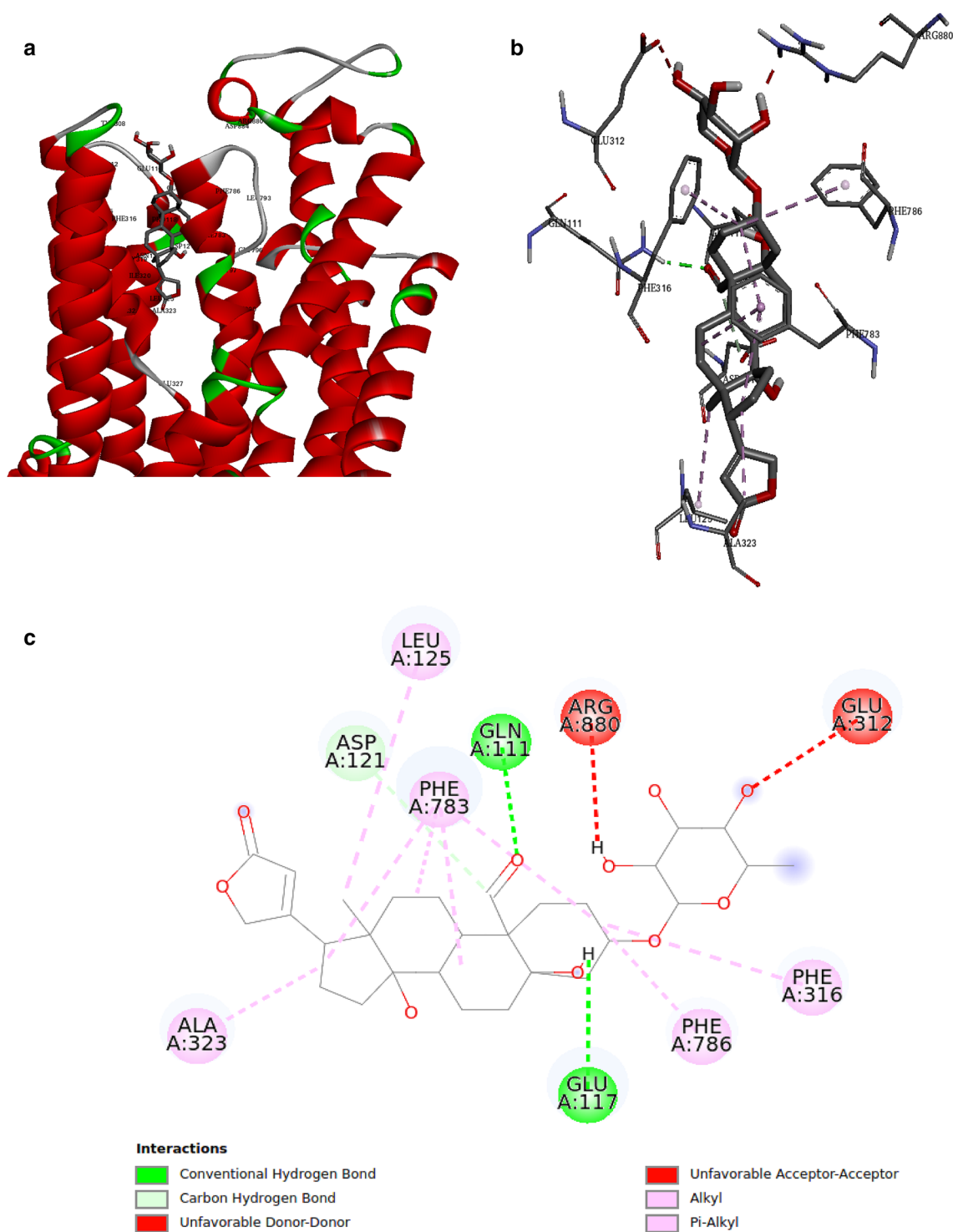


Fig. 6 Na,K-ATPase complexed with CON. **a** Close-up view of the binding site of human model (*solid* ribbons representation) with CON (tube representation). **b** 3D representation of the binding site of

Na,K-ATPase complexed with CON. **c** 2D pharmacophoric diagram between CON and Na,K-ATPase. The non-polar hydrogen was omitted for better visualization. (Color figure online)

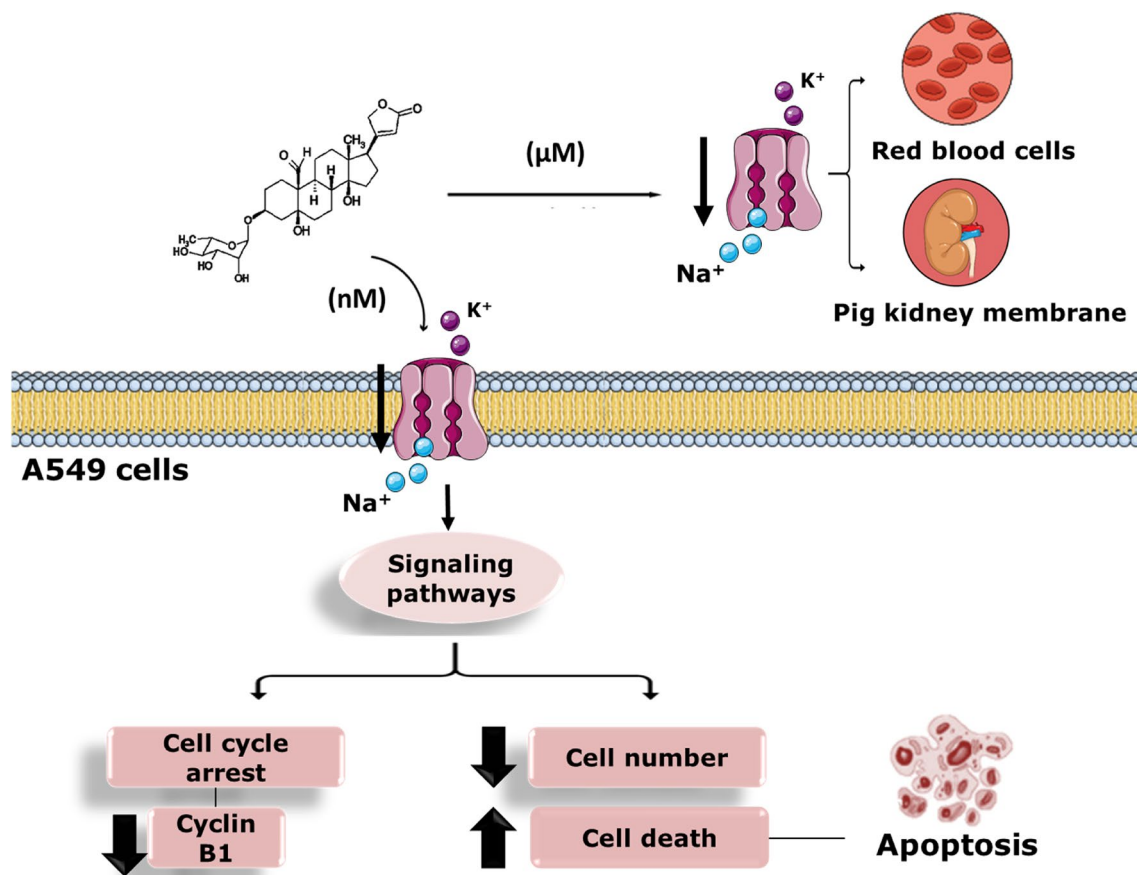


Fig. 7 CON induced cytostatic and cytotoxic effects in A549 cells, showing essentially apoptotic cell death. In addition, it prompted cell cycle arrest in G2/M and reduced cyclin B1 expression. CON also inhibited the Na,K-ATPase in A549 cells at nM concentrations. How-

ever, at the same concentrations, CON was unable to directly inhibit the Na,K-ATPase, either in pig kidney or in *red blood cells*. (Color figure online)

seven cardenolides, including CON, revealed that their potent cytotoxicity is associated to the presence of a monoglycoside unit at C3 and an aldehyde function at C10 on the aglycone [19].

Additionally, the structural differences among cardenolides *cis-trans-cis* steroids could interfere with binding properties of Na,K-ATPase, and also appear to alter subsequent signaling cascades. For example, several facts suggest that the DNA topoisomerases might be involved in the anticancer activity of cardiac glycosides, including ouabain, digoxin, and proscillaridin A in breast cancer MCF-7 cells. Several topoisomerase inhibitors currently used in the clinic (e.g., etoposide and camptothecin derivatives) have a lactone moiety, which seems to be crucial for their anticancer effects [57]. In this way, it is possible that CON modulated the activity of topoisomerase II prior to the induction of apoptosis. However, cardenolides effects in topoisomerase II on lung cancer cells have not been reported in the literature so far and should be better investigated.

Next, we tested whether CON inhibits Na,K-ATPase enzyme activity. This enzyme plays essential roles in ionic homeostasis and the regulation of diverse cell signaling events, including apoptosis, by binding to cardenolides [7]. The docking experiments confirmed that CON binds with high efficiency to the M1, M2, M4, M5, and extracellular M7-8 transmembrane. Although CON shows high binding energy in docking, this cannot be directly associated with a potent inhibitory effect of the pump. Based on these results, Weigand [58] tested the binding affinities of CON and ouabain to the $\alpha 1$ and 2 isoforms, and found similar binding affinities.

CON treatment is able to cause direct inhibition of pig kidney and human erythrocyte only at high concentrations (500 nM and 1 μM , respectively). However, lower concentrations (5–10 nM) were needed to inhibit the Na,K-ATPase in intact cells, at a range of concentrations similar to those required for the cytostatic effects in A549 cells. Other cardenolides presented similar effects on

membrane preparations and in intact cells, showing the possibility of the modulation of Na,K-ATPase expression in the cell membrane [59].

It is likely that the ability of CON to inhibit the Na,K-ATPase at low concentrations in A549 cells is dependent on the modulation levels of the enzyme in the membrane, and not on the direct inhibition. A549 cells expressed $\alpha 1$, $\alpha 2$, and $\alpha 3$ isoforms of Na,K-ATPase [60]. Even though the affinity of the isoforms in humans is similar, there is little information about the specific signaling pathways modulated by the different isoforms. It has been demonstrated that the $\alpha 2$ isoform is not able to activate ERK1/2 and Src [61, 62]. Another important fact is that cells that have low or no expression of $\alpha 3$ isoform are almost insensitive to the effect of ouabain, and the specific ratio between $\alpha 1$: $\alpha 3$ may be important to determine the sensitivity for cardiotonic steroid drugs [60].

The lack of correlation between these two Na,K-ATPase activity models prompts discussion of how CON affects this enzyme. These results appear not to be linked to the classical alterations in pumping activity, the positive inotropic effect that causes an increase in intracellular calcium, but rather, to the stimulation of the non-pumping pool of Na,K-ATPase, which in turn activates intracellular signaling pathways [8, 63].

Conclusion

In conclusion, we showed that CON possesses cytotoxic properties. A549 cells treated with this cardenolide undergo death, as evidenced by loss of membrane integrity, nucleus shrinkage, phosphatidylserine exposure, and caspase induction evidenced by z-VAD protection. Moreover, we showed, that CON induced G2/M phase arrest and cyclin B1 down-regulation. At a long term, CON also induces senescence in A549 cells. It also proved to be a Na,K-ATPase inhibitor, and the nature of this mechanism, such as signal transduction by protein–protein interactions, is a matter that deserves further investigation in this cell line. Taken together, our findings suggest that CON might work as an antitumor agent to help prevent lung cancer (Fig. 7).

Acknowledgements The Brazilian authors would like to thank the funding agencies CAPES /MEC (Ministry of Education) and CNPq/MCTI (Ministry of Science, Technology and Innovation) for their research scholarships. This work was also supported by the CNPq [Grants 472544/2013-6 and 490057/2011-0], the Marie Curie Foundation—IRSES/European Community [Grant 295251], and CAPES [Grant PNPd 2257/2011].

References

1. Siegel RL, Miller KD, Jemal A (2015) Cancer statistics, 2015. *CA Cancer J Clin* 65:5–29. doi:10.3322/caac.21254
2. Koh PK, Faivre-Finn C, Blackhall FH, De Ruysscher D (2012) Targeted agents in non-small cell lung cancer (NSCLC): clinical developments and rationale for the combination with thoracic radiotherapy. *Cancer Treat Rev* 38:626–640. doi:10.1016/j.ctrv.2011.11.003
3. Holohan C, Van Schaeybroeck S, Longley DB, Johnston PG (2013) Cancer drug resistance: an evolving paradigm. *Nat Rev Cancer* 13:714–726. doi:10.1038/nrc3599
4. Cragg GM, Newman DJ (2013) Natural products: a continuing source of novel drug leads. *Biochim Biophys Acta* 1830:3670–3695. doi:10.1016/j.bbagen.2013.02.008
5. Newman DJ, Cragg GM (2016) Natural products as sources of new drugs from 1981 to 2014. *J Nat Prod* 75:311–335. doi:10.1021/np200906s
6. Winnicka K, Bielawski K, Bielawska A (2006) Cardiac glycosides in cancer research. *Acta Pol Pharm* 63:109–115
7. Newman RA, Yang P, Pawlus AD, Block KI (2008) Cardiac glycosides as novel cancer therapeutic agents. *Mol Interv* 8:36–49. doi:10.1124/mi.8.1.8
8. Cerella C, Dicato M, Diederich M (2013) Assembling the puzzle of anti-cancer mechanisms triggered by cardiac glycosides. *Mitochondrion* 13:225–234. doi:10.1016/j.mito.2012.06.003
9. Mijatovic T, Van Quaquebeke E, Delest B et al (2007) Cardiotonic steroids on the road to anti-cancer therapy. *Biochim Biophys Acta* 1776:32–57. doi:10.1016/j.bbcan.2007.06.002
10. Wang Y, Qiu Q, Shen J-J et al (2012) Cardiac glycosides induce autophagy in human non-small cell lung cancer cells through regulation of dual signaling pathways. *Int J Dev Biol* 44:1813–1824. doi:10.1016/j.biocel.2012.06.028
11. Felth J, Rickardson L, Rosén J et al (2009) Cytotoxic effects of cardiac glycosides in colon cancer cells, alone and in combination with standard chemotherapeutic drugs. *J Nat Prod* 72:1969–1974. doi:10.1021/np900210m
12. Cerella C, Muller F, Gaigneaux A et al (2015) Early down-regulation of Mcl-1 regulates apoptosis triggered by cardiac glycoside UNBS1450. *Cell Death Dis* 6:e1782. doi:10.1038/cddis.2015.134
13. Chanvorachote P, Pongrakhananon V (2013) Ouabain downregulates Mcl-1 and sensitizes lung cancer cells to TRAIL-induced apoptosis. *Am J Physiol Cell Physiol* 304:263–272. doi:10.1152/ajpcell.00225.2012
14. Elbaz HA., Stueckle TA., Wang HYL et al (2012) Digitoxin and a synthetic monosaccharide analog inhibit cell viability in lung cancer cells. *Toxicol Appl Pharmacol* 258:51–60. doi:10.1016/j.taap.2011.10.007
15. Pongrakhananon V, Stueckle TA, Wang HL et al (2014) Monosaccharide digitoxin derivative sensitize human non-small cell lung cancer cells to anoikis through Mcl-1 proteasomal degradation. *Biochem Pharmacol* 88:23–35. doi:10.1016/j.bcp.2013.10.027
16. Hong DS, Henary H, Falchook GS et al (2014) First-in-human study of pbi-05204, an oleander-derived inhibitor of akt, fgf-2, nf- κ B and p70s6k, in patients with advanced solid tumors. *Invest New Drugs* 32:1204–1212. doi:10.1007/s10637-014-0127-0
17. Schneider NFZ, Geller FC, Persich L et al (2016) Inhibition of cell proliferation, invasion and migration by the cardenolides digitoxigenin monodigitoxoside and convallatoxin in human lung cancer cell line. *Nat Prod Res* 30:1327–1331. doi:10.1080/14786419.2015.1055265
18. Yang SY, Kim NH, Cho YS et al (2014) Convallatoxin, a dual inducer of autophagy and apoptosis, inhibits angiogenesis

- in vitro and in vivo. *PLoS ONE* 9:e91094. doi:[10.1371/journal.pone.0091094](https://doi.org/10.1371/journal.pone.0091094)
19. Levrier C, Kiremire B, Guéritte F, Litaudon M (2012) Toxicaric acid M, a new cytotoxic 10 β -hydroxy-19-nor-cardenolide from *Antiaris toxicaria*. *Fitoterapia* 83:660–664. doi:[10.1016/j.fitote.2012.02.001](https://doi.org/10.1016/j.fitote.2012.02.001)
 20. Prassas I, Karagiannis GS, Batruch I et al (2011) Digitoxin-induced cytotoxicity in cancer cells is mediated through distinct kinase and interferon signaling networks. *Mol Cancer Ther* 10:2083–2093. doi:[10.1158/1535-7163.MCT-11-0421](https://doi.org/10.1158/1535-7163.MCT-11-0421)
 21. Babula P, Masarik M, Adam V et al (2013) From Na⁺/K⁺-ATPase and cardiac glycosides to cytotoxicity and cancer treatment. *Anticancer Agents Med Chem* 13:1069–1087. doi:[10.2174/18715206113139990304](https://doi.org/10.2174/18715206113139990304)
 22. Jorgensen PL, Håkansson KO, Karlsh SJD (2003) Structure and Mechanism of Na, K-ATPase: functional sites and their interactions. *Annu Rev Physiol* 65:817–849. doi:[10.1146/annurev.physiol.65.092101.142558](https://doi.org/10.1146/annurev.physiol.65.092101.142558)
 23. Blanco G, Mercer RW (1998) Isozymes of the Na-K-ATPase: heterogeneity in structure, diversity in function. *Am J Physiol* 275:F633–F650. doi:[10.1152/ajprenal.00721.2010](https://doi.org/10.1152/ajprenal.00721.2010)
 24. Khan MI, Chesney JA, Laber DA, Miller DM (2009) Digitalis, a targeted therapy for cancer? *Am J Med Sci* 337:355–359. doi:[10.1097/MAJ.0b013e3181942f57](https://doi.org/10.1097/MAJ.0b013e3181942f57)
 25. Mijatovic T, Kiss R (2013) Cardiotoxic steroids-mediated Na⁺/K⁺-ATPase targeting could circumvent various chemoresistance pathways. *Planta Med* 79:189–198. doi:[10.1055/s-0032-1328243](https://doi.org/10.1055/s-0032-1328243)
 26. Cerejido M, Contreras RG, Shoshani L, Larre I (2012) The Na, K-ATPase as self-adhesion molecule and hormone receptor. *Am J Physiol Cell Physiol* 302:C473–C481. doi:[10.1152/ajpcell.00083.2011](https://doi.org/10.1152/ajpcell.00083.2011)
 27. Strober W (2001) Trypan blue exclusion test of cell viability. *Curr Protoc Immunol*. doi:[10.1002/0471142735.ima03bs21](https://doi.org/10.1002/0471142735.ima03bs21)
 28. Franken NAP, Rodermond HM, Stap J et al (2006) Clonogenic assay of cells in vitro. *Nat Protoc* 1:2315–2319. doi:[10.1038/nprot.2006.339](https://doi.org/10.1038/nprot.2006.339)
 29. Filippi-Chiela EC, Oliveira MM, Jurkovski B et al (2012) Nuclear morphometric analysis (NMA): screening of senescence, apoptosis and nuclear irregularities. *PLoS ONE*. doi:[10.1371/journal.pone.0042522](https://doi.org/10.1371/journal.pone.0042522)
 30. Riccardi C, Nicoletti I (2006) Analysis of apoptosis by propidium iodide staining and flow cytometry. *Nat Protoc* 1:1458–1461. doi:[10.1038/nprot.2006.238](https://doi.org/10.1038/nprot.2006.238)
 31. Henry CM, Hollville E, Martin SJ (2013) Measuring apoptosis by microscopy and flow cytometry. *Methods* 61:90–97. doi:[10.1016/j.ymeth.2013.01.008](https://doi.org/10.1016/j.ymeth.2013.01.008)
 32. Silva AO, Felipe KB, Villodre ES et al (2016) A guide for the analysis of long-term population growth in cancer. *Tumor Biol* 37:13743–13749. doi:[10.1007/s13277-016-5255-z](https://doi.org/10.1007/s13277-016-5255-z)
 33. Stewart JJP (2013) Optimization of parameters for semiempirical methods VI: more modifications to the NDDO approximations and re-optimization of parameters. *J Mol Model* 19:1–32. doi:[10.1007/s00894-012-1667-x](https://doi.org/10.1007/s00894-012-1667-x)
 34. Stewart JJP (2012) Stewart computational chemistry. MOPAC2012. <http://OpenMOPAC.net>
 35. Laursen M, Yatime L, Nissen P, Fedosova NU (2013) Crystal structure of the high-affinity Na⁺ + K⁺-ATPase-ouabain complex with Mg²⁺ bound in the cation binding site. *Proc Natl Acad Sci USA* 110:10958–10963. doi:[10.1073/pnas.1222308110](https://doi.org/10.1073/pnas.1222308110)
 36. Jaghoori MM, Bleijlevens B, Olabarriaga SD (2016) 1001 ways to run AutoDock Vina for virtual screening. *J Comput Aided Mol Des* 30:237–249. doi:[10.1007/s10822-016-9900-9](https://doi.org/10.1007/s10822-016-9900-9)
 37. Rocha SC, Pessoa MTC, Neves LDR et al (2014) 21-benzylidene digoxin: a proapoptotic cardenolide of cancer cells that up-regulates Na, K-ATPase and epithelial tight junctions. *PLoS ONE* 9:e108776. doi:[10.1371/journal.pone.0108776](https://doi.org/10.1371/journal.pone.0108776)
 38. Trott O, Olson A (2010) NIH public access. *J Comput Chem* 31:455–461. doi:[10.1002/jcc.21334](https://doi.org/10.1002/jcc.21334)
 39. Accelrys Software Inc (2013) Discovery studio modeling environment, release 4.5.
 40. Jorgensen P (1974) Purification and characterization of (Na⁺ + K⁺)-ATPase. 3. Purification from the outer medulla of mammalian kidney after selective removal of membrane components by sodium dodecylsulphate. *Biochim Biophys Acta* 12:36–52
 41. Jensen BYJ, Nrbj JG, Ottolenghi P (1984) Binding of sodium and potassium to the sodium pump of pig kidney evaluated from nucleotide-binding behaviour. *J Physiol* 346:219–241
 42. Sousa L, Garcia IJP, Costa TGF et al (2015) Effects of iron overload on the activity of Na, K-ATPase and lipid profile of the human erythrocyte membrane. *Plos ONE* 10:e0132852. doi:[10.1371/journal.pone.0132852](https://doi.org/10.1371/journal.pone.0132852)
 43. Fiske C, Subbarow Y (1925) The colorimetric determination of phosphorus. *J Biol Chem* 66:375–400
 44. Noël F, Pimenta PHC, Dos Santos AR et al (2011) Δ 2,3-ivermectin ethyl secoester, a conjugated ivermectin derivative with leishmanicidal activity but without inhibitory effect on mammalian P-type ATPases. *Naunyn-Schmiedeberg's Arch Pharm* 383:101–107. doi:[10.1007/s00210-010-0578-6](https://doi.org/10.1007/s00210-010-0578-6)
 45. Klaus B (2016) Statistical relevance—relevant statistics, part II⁺: presenting experimental data. *EMBO J* 35:1–4. doi:[10.15252/embj.201694659](https://doi.org/10.15252/embj.201694659)
 46. Liu Q, Tang J-S, Hu M-J et al (2013) Antiproliferative cardiac glycosides from the latex of *Antiaris toxicaria*. *J Nat Prod* 76:1771–1780. doi:[10.1021/np4005147](https://doi.org/10.1021/np4005147)
 47. Shi LS, Kuo SC, Sun HD et al (2014) Cytotoxic cardiac glycosides and coumarins from *Antiaris toxicaria*. *Bioorg Med Chem* 22:1889–1898. doi:[10.1016/j.bmc.2014.01.052](https://doi.org/10.1016/j.bmc.2014.01.052)
 48. Kuete V, Vouffo B, Mbaveng AT et al (2009) Evaluation of *Antiaris africana* methanol extract and compounds for antioxidant and antitumor activities. *Pharm Biol* 47:1042–1049. doi:[10.3109/13880200902988595](https://doi.org/10.3109/13880200902988595)
 49. Kaushik V, Yakisich J, Azad N et al (2016) Anti-tumor effects of cardiac glycosides on human lung cancer cells and lung tumorspheres. *J Cell Physiol*. doi:[10.1002/jcp.25611](https://doi.org/10.1002/jcp.25611)
 50. Zhou S, Zhao L, Kuang M et al (2012) Autophagy in tumorigenesis and cancer therapy: Dr. Jekyll or Mr. Hyde? *Cancer Lett* 323:115–127. doi:[10.1016/j.canlet.2012.02.017](https://doi.org/10.1016/j.canlet.2012.02.017)
 51. Leu WJ, Chang HS, Chan SH et al (2014) Reevesioside A, a cardenolide glycoside, induces anticancer activity against human hormone-refractory prostate cancers through suppression of c-myc expression and induction of G1 arrest of the cell cycle. *PLoS ONE* 9:1–13. doi:[10.1371/journal.pone.0087323](https://doi.org/10.1371/journal.pone.0087323)
 52. Lapenna S, Giordano A (2009) Cell cycle kinases as therapeutic targets for cancer. *Nat Rev Drug Disc* 8:547–566. doi:[10.1038/nrd2907](https://doi.org/10.1038/nrd2907)
 53. Van Quaquebeke E, Simon G, RE A et al (2005) Identification of a novel cardenolide (2''-oxovoruscharin) from *Calotropis procera* and the hemisynthesis of novel derivatives displaying potent in vitro antitumor activities and high in vivo tolerance: structure–activity relationship analyses. *J Med Chem* 48:849–856. doi:[10.1021/jm049405a](https://doi.org/10.1021/jm049405a)
 54. Juncker T, Cerella C, Teiten M et al (2011) UNBS1450, a steroid cardiac glycoside inducing apoptotic cell death in human leukemia cells. *Biochem Pharmacol* 81:13–23. doi:[10.1016/j.bcp.2010.08.025](https://doi.org/10.1016/j.bcp.2010.08.025)
 55. Feng B, Guo Y-W, Huang C-G et al (2010) 2'-epi-2'-O-acetylthevetin B extracted from seeds of *Cerbera manghas* L. induces cell cycle arrest and apoptosis in human hepatocellular carcinoma HepG2 cells. *Chem Biol Interact* 183:142–153. doi:[10.1016/j.cbi.2009.10.012](https://doi.org/10.1016/j.cbi.2009.10.012)

56. Kulikov A, Eva A, Kirch U et al (2007) Ouabain activates signaling pathways associated with cell death in human neuroblastoma. *Biochim Biophys Acta* 1768:1691–1702. doi:[10.1016/j.bbamem.2007.04.012](https://doi.org/10.1016/j.bbamem.2007.04.012)
57. Bielawski K, Winnicka K, Bielawska A (2006) Inhibition of DNA topoisomerases I and II, and growth inhibition of breast cancer MCF-7 cells by ouabain, digoxin and proscillaridin A. *Biol Pharm Bull* 29:1493–1497
58. Weigand KM, Laursen M, Swarts HGP et al (2014) Na⁺,K⁺-ATPase isoform selectivity for digitalis-like compounds is determined by two amino acids in the first extracellular loop. *Chem Res Toxicol* 27:2082–2092. doi:[10.1021/tx500290k](https://doi.org/10.1021/tx500290k)
59. Alves SLG, Paixão N, Ferreira LGR et al (2015) c-Benzylidene digoxin derivatives synthesis and molecular modeling[†]: evaluation of anticancer and the Na, K-ATPase activity effect. *Bioorg Med Chem* 23:4397–4404. doi:[10.1016/j.bmc.2015.06.028](https://doi.org/10.1016/j.bmc.2015.06.028)
60. Trenti A (2012) Analysis of the molecular mechanisms of the antineoplastic effect of ouabain. Università degli Studi di Padova
61. Pierre SV, Sottejeau Y, Gourbeau J et al (2008) Isoform specificity of Na-K-ATPase-mediated ouabain signaling. *Am J Physiol Renal Physiol* 1:859–866. doi:[10.1152/ajprenal.00089.2007](https://doi.org/10.1152/ajprenal.00089.2007)
62. Xie J, Ye Q, Cui X et al (2015) Expression of rat Na-K-ATPase alpha 2 enables ion pumping but not ouabain-induced signaling in alpha1-deficient porcine renal epithelial cells. *Am J Physiol Cell Physiol* 309:C373–C382. doi:[10.1152/ajpcell.00103.2015](https://doi.org/10.1152/ajpcell.00103.2015)
63. Slingerland M, Cerella C, Guchelaar HJ et al (2013) Cardiac glycosides in cancer therapy: from preclinical investigations towards clinical trials. *Invest New Drugs* 31:1087–1094. doi:[10.1007/s10637-013-9984-1](https://doi.org/10.1007/s10637-013-9984-1)